Applied Physics Letters

RESEARCH ARTICLE | NOVEMBER 17 2022

Small-polaron conductivity in perovskite ferroelectric $BaTiO_3$ films

M. Tyunina ; M. Savinov; A. Dejneka

Appl. Phys. Lett. 121, 202901 (2022)
https://doi.org/10.1063/5.0129831

Applied Physics Letters ARTICLE scitation.org/journal/apl

Small-polaron conductivity in perovskite ferroelectric $BaTiO_3$ films

Cite as: Appl. Phys. Lett. **121**, 202901 (2022); doi: 10.1063/5.0129831
Submitted: 7 October 2022 · Accepted: 7 November 2022 ·
Published Online: 17 November 2022

M. Tyunina,[1,2,a)] M. Savinov,[2] and A. Dejneka[2]

AFFILIATIONS

[1]Microelectronics Research Unit, Faculty of Information Technology and Electrical Engineering, University of Oulu, P. O. Box 4500, FI-90014 Oulu, Finland
[2]Institute of Physics of the Czech Academy of Sciences, Na Slovance 2, 18221 Prague, Czech Republic

[a)]Author to whom correspondence should be addressed: marina.tjunina@oulu.fi

ABSTRACT

In ABO_3 perovskite oxide ferroelectrics, electrical conductivity ranges from insulator- to superconductor-type and is virtually critical for all applications of these materials. Compared to bulk ceramics and crystals, ferroelectric thin films can enable advanced control of the conductivity. Here, small-polaron hopping conductivity was evidenced and examined in various pulsed-laser-deposited films of ferroelectric $BaTiO_3$ and reference films of $SrTiO_3$. For this, AC conductivity was studied in a broad range of temperatures and frequencies for films sandwiched between the bottom and top electrodes. In the $BaTiO_3$ films, with increasing temperature, a significant increase in activation energy for small-polaron hopping was found and ascribed to strong electron–phonon coupling and complex lattice oscillations therein. Plain relations of the activation energy to microstructure, composition, or phase transitions were lacking, which corroborated the critical role of phonons. Additionally, a phonon-less transport was detected. It was anticipated that owing to strong electron–phonon coupling, rich phonon ensembles, and coexistence of phonon-stimulated and phonon-less processes, the small-polaron conductivity can heavily vary in ferroelectric films that necessitates further studies.

Barium titanate ($BaTiO_3$ or BTO) is an archetypal representative of ABO_3 perovskite oxide ferroelectrics (FEs). Very large dielectric permittivity and strong electromechanical and electro-optical effects in FEs enable important FE applications in the diverse fields of electronics and photonics. FEs are fundamentally wide-bandgap insulators and normally display negligibly small electrical conductivity, which is beneficial for mainstream FE devices. In addition, FEs hold good potential for photovoltaics, catalysis, resistive switching, and other innovations, where increased conductivity is desirable. Such enhanced conductivity is usually achieved using appropriate cationic doping and/or removal, or replacement, of oxygen. Furthermore, very large low-temperature conductivity [including superconductivity as demonstrated in doped $SrTiO_3$ (STO)] can arise from strong electron–phonon coupling and related formation of large (Fröhlich-type) polarons in FEs. Thus, FEs can host a variety of electronic states ranging from insulators to superconductors. Controlling these states and the electrical conductivity is pivotal for virtually all modern, emerging, and viable future FE devices.

As compared to bulk ceramics and crystals, FE thin films enable not only advanced applications but also unusual, film-specific possibilities to tailor the properties. In particular, the nonequilibrium process of pulsed laser deposition (PLD) ensures growth of perovskite-structure films, where remarkably large amounts of oxygen are removed and/or replaced *in situ* during deposition. Recently, we demonstrated several such PLD-grown films with up to 10% of oxygen atoms being removed/replaced.[1–5] We also showed that contrary to large semiconductor- or metal-like conductivity in reduced bulk FEs, the PLD-grown anion-modified films exhibited an excellent insulating behavior in a broad temperature range of up to 500 K.[6–8] Detailed studies of AC conductivity revealed the hopping mechanism of charge transport therein. The main charge carriers were suggested to be small (Holstein-like) polarons.

In FEs, formation of small self-trapped electron polarons, mostly localized on the *B*-type ions, was theoretically justified.[9–13] The electron (hole) localization may be enhanced in the presence of oxygen vacancies/substitutions as well as promoted by FE polarization or lattice strain. Because of strong charge carrier localization, small-polaron transport is realized by hopping, and DC conductivity increases with temperature due to the temperature-dependent mobility μ_H,

$$\mu_H \propto T^{-1}\exp\left(-\frac{E_H}{k_B T}\right). \quad (1)$$

Here, k_B is the Boltzmann constant, and the hopping activation energy E_H is often roughly estimated as half binding energy of small polarons.[14,15] As seen from (1), large enough E_H can determine colossal changes of conductivity with temperature and/or electric field. Thus, mastering E_H may facilitate desired conductivity and, furthermore, enable unprecedented effects and applications based thereon.

In this work, we focused on closer inspection of the small-polaron transport in the PLD-grown BTO films. We acquired and analyzed AC conductivity datasets, which are sufficient to accurately determine the energy E_H. First, we scrutinized conductivity in oxygen-deficient BTO films, including epitaxial and polycrystalline ones. We observed a significant increase in E_H with temperature. We considered theoretical polaron mobility and showed that such a behavior of $E_H(T)$ can arise from strong electron–phonon coupling and complex temperature-dependent phonon ensemble in BTO. By comparing $E_H(T)$ in different BTO and reference $SrTiO_3$ (STO) films, we discarded the direct effects of phase transitions, microstructure, or composition on E_H. Additionally, by inspecting the frequency dispersion of the AC conductivity, we detected the presence of phonon-less transport in the films. Our observations suggest that peculiar electron–phonon coupling, ample phonons, and coexistence of phonon-mediated and phonon-less processes can lead to massive variations in the small-polaron conductivity in FE films. Thorough investigations are needed to comprehend such variations and bring them to fruition.

We primarily investigated the conductivity in thin (80 nm) epitaxial and polycrystalline BTO films, which were grown within a single PLD process, thus ensuring similar chemical composition for both films. With an oxygen pressure of 5 Pa, we achieved a perfect epitaxial *c*-type BTO film on the (001) STO substrate with a $SrRuO_3$ (SRO) bottom electrode,[16] whereas randomly oriented polycrystalline BTO grew on Pt-coated Si substrates (supplementary material Fig. S1). For comparison, we used 180-nm-thick epitaxial BTO films on SRO/(001)STO:[16,17] one was stoichiometric of *a*-type and another was oxygen-deficient and contained both the *c*-phase at the bottom and the *a*-phase on the top. As a reference, we selected a stoichiometric epitaxial cubic ($c = a$) STO film on SRO/(001)STO and oxygen-deficient epitaxial *c*-type STO films on a $LaNiO_3$-coated (001) $(LaAlO_3)_{0.3}(Sr_2AlTaO_6)_{0.7}$ substrate.[3,6]

For electrical characterization, Pt top electrodes were formed by PLD using a shadow mask. The impedance was measured by a Novocontrol Alpha-AN High Performance Frequency Analyzer, and the control of temperature was realized using Linkam cold/hot stages. The AC conductivity was investigated as a function of temperature $T = 80$–500 K and frequency $f = 1$–10^6 Hz and using the amplitude of the AC probing signal $V_{AC} = 10^{-3}$ V. The measurements were performed on heating/cooling with the maximum temperature of 500 K. This regime ensured the lack of thermal hysteresis in comparison with the measurements for the maximum temperature of 700 K.[8] We stress that the conductivity was determined in the out-of-plane direction (normal to the substrate surface, i.e., along the longer unit-cell axis in the *c*-film and the shorter axis in the *a*-film), which contrasts with commonly studied in-plane sheet resistance. We also emphasize that the out-of-plane small-signal AC measurements eradicated (or minimized) the effects of charge injection, electric field, and surface (interface) conductivity.

The out-of-plane AC conductivity σ, measured in the 80-nm thick oxygen deficient BTO films, is presented as a function of frequency f for different temperatures T in Figs. 1(a) and 1(e). Both

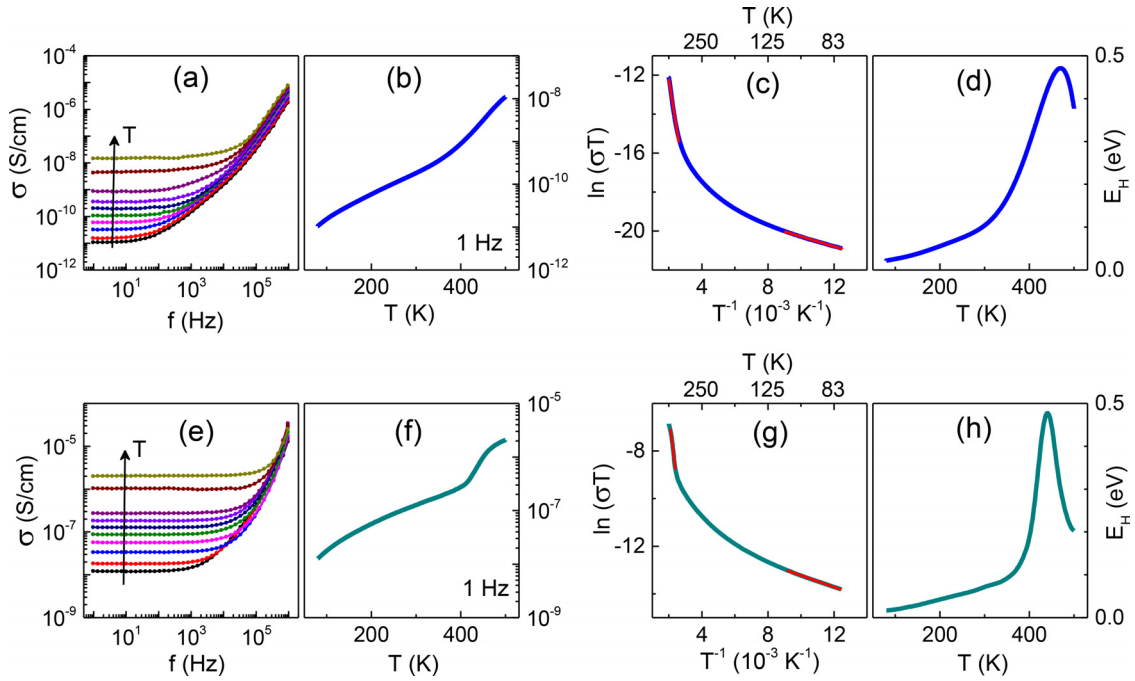

FIG. 1. (a) and (e) Log–log plots of conductivity as a function of frequency at $T = 80$–500 K (arrows show directions of temperature increase); (b) and (f) semi-log plots of conductivity as a function of temperature at $f = 1$ Hz; (c) and (g) plots of $\ln(\sigma T)$ as a function of the inverse temperature (linear fits are also shown); and (d) and (h) hopping activation energy E_H as a function of temperature in the (a)–(d) *c*-type epitaxial and (e)–(h) polycrystalline BTO films.

BTO films, epitaxial and polycrystalline ones, exhibit a very small $\sigma \sim 10^{-11}$–10^{-8} S/cm at low T and f, implying good insulating properties. The conductivity $\sigma(f, T)$ increases strongly with frequency and/or temperature, which is consistent with the hopping mechanism[18]

$$\sigma(f, T) = \sigma_o(T) + \alpha(T) f^{s(T)} + \varepsilon'' f. \quad (2)$$

Here, σ_0 is the DC conductivity, the coefficient $\alpha(T)$ and the exponent $s(T)$ describe frequency dispersion of AC conductivity, and ε'' is the imaginary part of the dielectric permittivity. The measured conductivity is frequency-independent and, thus, dominated by the DC component at low frequencies ($f < 10$ Hz in epitaxial BTO and $f < 1$ kHz in polycrystalline BTO) [Figs. 1(a) and 1(e)]. Therefore, the data at $f = 1$ Hz are relevant for examining the hopping DC conductivity [Figs. 1(b) and 1(f)], which is generally proportional to $[T^{-m}\exp(-T^{-m})]$ with the parameter $m \leq 1$ being specific for a certain type of localization and transport. The obtained plots of $[\ln(\sigma T^m)]$ as a function of (T^{-m}) are not linear for any m, although several linear fractions may be retrieved by reducing temperature intervals for fits [Figs. 1(c) and 1(g) and supplementary material Fig. S2]. Such a behavior can indicate small-polaron transport ($m = 1$) with the temperature-dependent $E_H(T)$.[14,15] Then one can write

$$\ln(\sigma T) \propto -\left(\frac{E_H}{k_B}\right) \cdot \left(\frac{1}{T}\right), \quad (3)$$

$$E_H(T) = -k_B \cdot \frac{\partial[\ln(\sigma T)]}{\partial\left[\left(\frac{1}{T}\right)\right]}. \quad (4)$$

In accordance with (4), the energy E_H was extracted from the experimental data by differentiating the plots of $\ln(\sigma T)$ vs $1/T$ [in Figs. 1(c) and 1(g)] and presented as a function of temperature [Figs. 1(d) and 1(h)]. The energy E_H significantly increases with increasing temperature. Furthermore, there are two temperature regions with distinct paces of the energy increase and inflection between them at ~350–400 K. Interestingly, the energies $E_H(T)$ are nearly similar in both BTO films, although inflection is better expressed in the polycrystalline BTO.

To analyze the behavior $E_H(T)$, the theoretical (Holstein) small-polaron mobility μ_{SP} was calculated using the expression[14]

$$\mu_{SP} = \frac{ea^2 J^2}{k_B T \hbar^2 \omega_{OP}} \left[\frac{\pi}{\gamma \cosh\left(\frac{\hbar\omega_{OP}}{4k_B T}\right)}\right]^{\frac{1}{2}} \exp\left[-2\gamma \tanh\left(\frac{\hbar\omega_{OP}}{4k_B T}\right)\right], \quad (5)$$

where e is the elementary charge, a is the lattice constant, J is the overlap integral, ω_{OP} is the frequency of optical phonons, and γ is the electron–phonon coupling constant. The calculations of μ_{SP} for $ea^2J^2 = 1$ and varying ω_{OP} (from 67 to 670 cm^{-1}) and γ (from 5 to 20) show that the magnitude and the temperature dependence of μ_{SP} dramatically change with ω_{OP} and/or γ [Fig. 2(a)]. The curves [$\ln(\mu_{SP}T)$ vs $1/T$] can be linear for the smallest parameters ω_{OP} and γ only [Fig. 2(b)]. Correspondingly, the energy E_H, extracted by differentiating [$\ln(\mu_{SP}T)$ vs $1/T$], is small and nearly constant for the smallest parameters ω_{OP} and γ but is significantly larger and increases with temperature for larger ω_{OP} and/or γ [Figs. 2(c) and 2(d)].

Based on the results in Fig. 2, the behavior $E_H(T)$ in BTO [Figs. 1(d) and 1(h)] can be ascribed to the high frequency of optical phonons involved in hopping, strong electron–phonon coupling, and increase in ω_{OP} and/or γ on heating above ~350–400 K. Because of complex lattice oscillations in BTO,[19–23] it is difficult to explicitly assign ω_{OP} as well as to follow changes in ω_{OP} and γ with temperature. We note that the crystal structure, spontaneous polarization, phonon frequencies, and electron–phonon coupling change concurrently at the para (PE)-to-FE (and FE-to-FE) phase transitions. In the polycrystalline BTO film, the PE–FE transition may, indeed, lead to the inflection in $E_H(T)$, whose temperature of ~400 K coincides with the temperature of the PE–FE transition, confirmed by the peak in the dielectric permittivity (supplementary material Fig. S3). However, this is not valid for the epitaxial c-BTO film, where the PE–FE transition occurs at $T > 500$ K and dielectric anomalies are absent at ~350 K (supplementary material Fig. S4).[8] In search of an explanation, we inspected $E_H(T)$ in different epitaxial BTO films and detected an apparent microstructural effect [Fig. 3(a)]. Compared to the pronounced inflection of $E_H(T)$ in the c-BTO film, the inflection is smeared in the a-BTO film, whereas an intermediate behavior is observed in the c–a BTO film. Again, this microstructural effect does not stand for epitaxial STO films [Fig. 3(b)]: in the studied temperature range, the energies E_H are practically similar in the stoichiometric cubic film ($c = a$) and the oxygen-deficient c-tetragonal film [Fig. 3(b)]. The observed absence of direct relations of the energy E_H to microstructure, composition, or phase transitions is coherent with the critical role of phonons, whose parameters (ω_{OP}, γ) are unknown and may alter in a complex manner. Despite the lack of clear correlations and understanding, the obtained results, nevertheless, imply that the energy E_H can immensely vary in FE films.

We note that whereas phonons are involved in small-polaron barrier hopping, phonon-less transport is also possible. Such transport

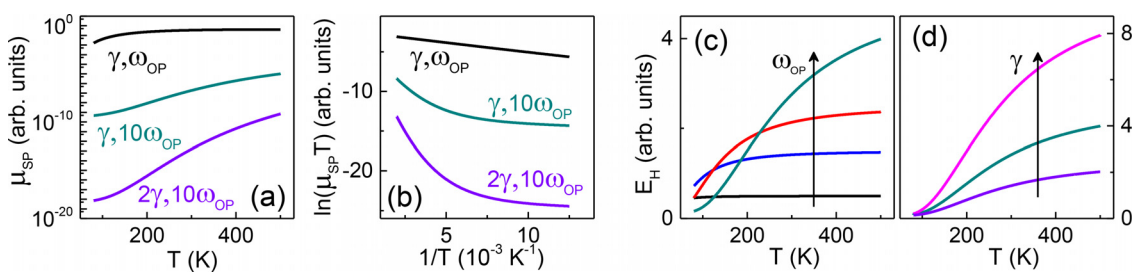

FIG. 2. Calculated (a) mobility μ_{SP} as a function of temperature and (b) $\ln(\mu_{SP}T)$ as a function of the inverse temperature. In (a) and (b), the parameters are $\omega_{OP} = 67$ cm^{-1} and $\gamma = 10$. (c) and (d) Activation energy E_H extracted from the calculations as a function of temperature. In (c), the parameters are $\omega_{OP} = 67$–670 cm^{-1} and $\gamma = 10$. In (d), the parameters are $\omega_{OP} = 670$ cm^{-1} and $\gamma = 5$, 10, and 20.

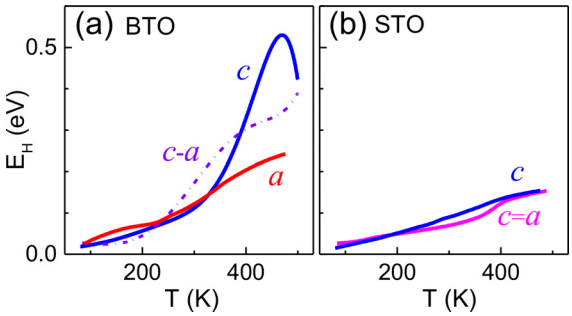

FIG. 3. Activation energy E_H as a function of temperature in different epitaxial films of (a) BTO and (b) STO.

cannot be identified from the temperature dependence of the DC conductivity. However, it can be manifested in the frequency-dependent AC conductivity [see expression (2)].[14,15,18,24] Roughly, the exponent $s(T)$ is $s < 1$ and decreases with temperature for thermally activated hopping. The exponent is temperature-independent and can take values of $s \leq 1$ for tunneling or $s \approx 2$ for resonance transport.[18] For an epitaxial *c*-BTO film, each plot of $\ln(\sigma)$ as a function of $\ln(f)$ comprises two distinct linear regions for any temperature [Fig. 4(a)]. The two corresponding fitted exponents are displayed in Fig. 4(b). One exponent is temperature-independent $\sim$1 for $T < 300$ K, which is difficult to unambiguously ascribe to tunneling because of possible concurrent contributions from the dielectric relaxation and barrier hopping at these temperatures. At $T > 300$ K, this exponent is <1 and decreases with increasing temperature, which is consistent with the temperature-activated hopping as seen in the DC behavior. Importantly, there is another exponent, which is large $\sim$1.7 and temperature-independent, and thus, evidence the presence of a phonon-less resonant transport. In the polycrystalline BTO film, the curves [$\ln(\sigma)$ vs $\ln(f)$] are parabolic (supplementary material Fig. S5), showing the presence of $s \approx 2$ and, hence, phonon-less processes as well. Thus, the phonon-stimulated and phonon-less processes of small-polaron transport coexist in the BTO films. Importantly, for many FE devices operating at relatively high frequencies or speeds, it is essential to control not only thermally activated but also phonon-less transport, which requires careful studies.

In summary, the electrical AC conductivity was examined in a broad range of temperatures (80–500 K) and frequencies (1 Hz–1 MHz) in various thin PLD-grown BTO and reference STO films sandwiched

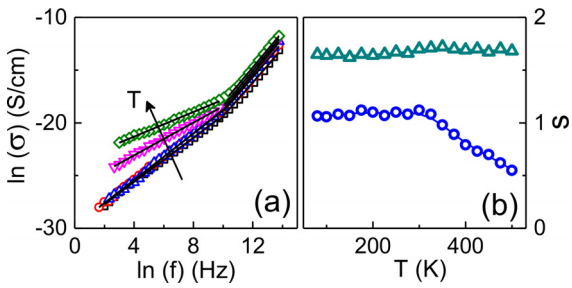

FIG. 4. (a) Logarithmic relationship between conductivity and frequency at $T = 100$, 200, 300, 400, and 500 K in the epitaxial *c*-BTO film. Straight lines are fits. Arrow shows the direction of temperature increase. (b) Exponents *s* extracted from the linear fits [$\ln(\sigma) \propto \ln(f)$] as a function of temperature.

between the bottom and top electrodes. The small-polaron hopping conductivity was evidenced and analyzed. The hopping activation energy significantly increased with temperature in the BTO films, which was ascribed to strong electron–phonon coupling and complex lattice oscillations in BTO. Due to the critical role of phonons, direct correlations of the activation energy with microstructure, composition, or phase transitions were absent. Additionally, the presence of phonon-less transport was detected. It was suggested that owing to peculiar electron–phonon coupling, manifold ensemble of phonons, and coexistence of phonon-mediated and phonon-less processes, the small-polaron conductivity can heavily vary in FE films and requires thorough further investigations.

See the supplementary material for (I) crystal orientation, (II) details of DC of conductivity, (III) dielectric permittivity, and (IV) frequency dispersion of AC conductivity.

The authors would like to thank T. Kocourek, O. Pacherova, S. Cichon, and V. Bijalwan for their assistance on different stages of the work. The authors acknowledge the support from the Czech Science Foundation (Grant No. 22-10832S) and the European Structural and Investment Funds and the Ministry of Education, Youth and Sports of the Czech Republic through Programme "Research, Development and Education" (Project No. SOLID21-CZ.02.1.01/0.0/0.0/16_019/0000760).

AUTHOR DECLARATIONS

Conflict of Interest

The authors have no conflicts to disclose.

Author Contributions

Marina Tyunina: Conceptualization (lead); Data curation (lead); Formal analysis (lead); Funding acquisition (equal); Investigation (equal); Methodology (equal); Project administration (equal); Writing – original draft (lead); Writing – review & editing (lead). **Maxim Savinov:** Data curation (equal); Investigation (equal); Methodology (equal); Software (equal). **Alexandr Dejneka:** Funding acquisition (equal); Project administration (equal); Resources (equal).

DATA AVAILABILITY

The data that support the findings of this study are available within the article and its supplementary material.

REFERENCES

[1]M. Tyunina, J. Levoska, O. Pacherova, T. Kocourek, and A. Dejneka, J. Mater. Chem. C **10**, 6770 (2022).
[2]M. Tyunina, O. Pacherova, T. Kocourek, and A. Dejneka, Sci. Rep. **11**, 15247 (2021).
[3]M. Tyunina, L. L. Rusevich, E. A. Kotomin, O. Pacherova, T. Kocourek, and A. Dejneka, J. Mater. Chem. C **9**, 1693 (2021).
[4]M. Tyunina, O. Vetokhina, N. Nepomniashchaia, O. Pacherova, S. Cichon, T. Kocourek, M. Jelinek, and A. Dejneka, APL Mater. **8**, 071107 (2020).
[5]M. Tyunina, O. Pacherova, N. Nepomniashchaia, V. Vetokhina, S. Cichon, T. Kocourek, and A. Dejneka, Phys. Chem. Chem. Phys. **22**, 24796 (2020).
[6]M. Tyunina, M. Savinov, and A. Dejneka, Appl. Phys. Lett. **119**, 192901 (2021).
[7]L. L. Rusevich, M. Tyunina, E. A. Kotomin, N. Nepomniashchaia, and A. Dejneka, Sci. Rep. **11**, 23341 (2021).

[8]M. Tyunina and M. Savinov, Phys. Rev. B **101**, 094106 (2020).
[9]R. I. Eglitis, E. A. Kotomin, and G. Borstel, J. Phys. **14**, 3735 (2002).
[10]E. A. Kotomin, R. I. Eglitis, and G. Borstel, J. Phys. **12**, L557 (2000).
[11]N. Tsunoda, Y. Kumagai, and F. Oba, Phys. Rev. Mater. **3**, 114602 (2019).
[12]T. Xu, T. Shimada, Y. Araki, M. Mori, G. Fujimoto, J. Wang, T.-Y. Zhang, and T. Kitamura, npj Comput. Mater. **5**, 23 (2019).
[13]A. Janotti, J. B. Varley, M. Choi, and C. G. Van de Walle, Phys. Rev. B **90**, 085202 (2014).
[14]A. S. Alexandrov and J. T. Devreese, *Advances in Polaron Physics* (Springer-Verlag, Berlin, Heidelberg, 2007).
[15]D. Emin, *Polarons* (Cambridge University Press, Cambridge, 2012).
[16]M. Tyunina, J. Peräntie, T. Kocourek, S. Saukko, H. Jantunen, M. Jelinek, and A. Dejneka, Phys. Rev. Res. **2**, 023056 (2020).
[17]M. Tyunina, O. Pacherova, J. Peräntie, M. Savinov, M. Jelinek, H. Jantunen, and A. Dejneka, Sci. Rep. **9**, 3677 (2019).
[18]*Charge Transport in Disordered Solids with Applications in Electronics*, edited by S. Baranovski (Wiley, New York, 2006).
[19]A. Scalabrin, A. S. Chaves, D. S. Shim, and S. P. S. Porto, Phys. Status Solidi B **79**, 731 (1977).
[20]I. B. Ouni, D. Chapron, H. Aroui, and M. D. Fontana, Appl. Phys. A **122**, 480 (2016).
[21]P. Ghosez, E. Cockayne, U. V. Waghmare, and K. M. Rabe, Phys. Rev. B **60**, 836 (1999).
[22]R. A. Evarestov and A. V. Bandura, J. Comput. Chem. **33**, 1123 (2012).
[23]V. Dwij, B. K. De, G. Sharma, D. K. Shukla, M. K. Gupta, R. Mittal, and V. Sathe, Physica B **624**, 413381 (2022).
[24]A. Ghosh, Phys. Rev. B **41**, 1479 (1990).